

# Hemodynamics Assessments of Ascending Thoracic Aortic Aneurysm – the Influence of Hematocrit with Fluid-Structure Interaction Analysis

Han Hung Yeh<sup>1,2</sup>, Simon W Rabkin<sup>3</sup> and Dana Grecov<sup>1,2,\*</sup>

<sup>1</sup> School of Biomedical Engineering, University of British Columbia, Vancouver, BC, Canada.

<sup>2</sup> Department of Mechanical Engineering, University of British Columbia, Vancouver, BC, Canada.

<sup>3</sup> Department of Medicine (Cardiology), University of British Columbia, Vancouver, BC, Canada.

\* 2054-6250 Applied Science Lane, Vancouver, BC V6T1Z4, Canada, dgrecov@mech.ubc.ca

**Abstract**— Aortic aneurysm is one of the cardiovascular diseases with localized abnormal growth of a blood vessel with a risk of rupture or dissect. The precise pathological pathway for disease progression in aneurysm formation is not completely understood. In the current study, ascending thoracic aortic aneurysms are investigated using fully coupled fluid-structure interaction method with the focus to investigate the importance of changes in hematocrit under normotension and hypertension. Blood was modelled as incompressible flow within laminar regime with the use of the Quemada model to account for the effect of hematocrits. The anisotropic hyperelastic properties of the aortic wall were considered. Given the change in the degree of shear thinning from the non-Newtonian behavior of blood due to the change in hematocrit, the simulated result could provide valuable information in clinical practice. Indeed, our results suggested that with the increase in hematocrit, the shear stress distribution as well as the maximum shear stress magnitude along the arterial wall would increase significantly. The arterial wall stress distributions, however, remained unchanged with respect to the changes in hematocrit.

**Keywords**— Ascending thoracic aortic aneurysm, fluid-structure interaction, hypertension, arterial wall deformation, hematocrit

## I. INTRODUCTION

Although genetics, gender, age, and smoking are the risk factors for aortic aneurysm progression, the precise reason for the development and expansion of an aneurysm is still uncertain for most cases [1]. Biomechanically, the most commonly used parameters for aneurysm managements are the aneurysm diameter and the patient's blood pressure. However, evaluating the risk based on the aneurysm diameter might not be sufficient as a smaller aneurysm may progress into an aortic dissection before the aneurysm grows to the recommended surgical threshold [2]. Unfortunately, during an evaluation of an aneurysm, other factors such as the aneurysm anatomy and the patient's hemorheological characteristics are not directly involved.

There are finite element simulations studying the effect of the wall stress within an aneurysm using patient-specific

data. The focuses for these studies were on mechanical stress of the arterial wall without the consideration of blood flow [3, 4] and they provide insights on the risk of dissection or rupture. The Fluid-structure interaction (FSI) method, which considers the coupled effect between the influence of fluid to solid and vice versa, has been used to investigate the influence of blood pressure on the aneurysm's wall stress in idealized ascending thoracic aortic aneurysms (ATAA) [5]. Additionally, different rheological models, including the Carreau, the Quemada, and the Cross model, could be integrated to account for the non-Newtonian behavior of blood. However, when considering investigations with clinically available and patient-specific information, the Quemada model, with hematocrit as an extra rheological parameter, provides an easier adaptation in practice.

Therefore, the main objective of the current study was to extend our previous ATAA investigation and determine the influence on the changes of hematocrit in the hemodynamics and arterial wall responses using fully coupled FSI method.

## II. METHOD

### A. Governing Equations

Current ATAAs were modelled with a fully-coupled FSI method to account for the interactions between laminar blood flow and anisotropic hyperelastic aortic wall [5,6]. The hemodynamics were governed by the incompressible Navier-Stokes equations with continuity (1) and momentum conservation equations (2). The gravitational force was assumed to be negligible due to small elevation. The coupling between the arterial wall and blood flow was achieved with the coupling equation (3) where Cauchy stress tensor,  $\sigma$ , was computed based on the fluid's pressure and the viscous stress from the momentum equations. To account for the anisotropy of arterial wall, the strain energy density function,  $\bar{\Psi}$ , is used to compute the arterial wall deformation based on the strain energy stored. Equation (4) is the summation of the isotropic and the anisotropic component, which accounts for both the hyperelastic neo-Hookean base and the collagen fibers.

$$\nabla \cdot \mathbf{V} = 0, \quad (1)$$

$$\rho \frac{D\mathbf{V}}{Dt} = \nabla \cdot (-P\mathbf{I} + \boldsymbol{\tau}), \quad (2)$$

$$\boldsymbol{\sigma} \cdot \mathbf{n} = (-P\mathbf{I} + \boldsymbol{\tau}) \cdot \mathbf{n}, \quad (3)$$

$$\bar{\Psi} = \frac{k_3}{2} (I_1 - 3) + \frac{k_1}{2k_2} \sum_{i=4,6} \{e^{[k_2(I_i-1)^2]} - 1\} \quad (4)$$

Where  $\mathbf{V}$  is the fluid velocity,  $\rho$  is the fluid density,  $P$  is the pressure,  $\mathbf{I}$  is the identity tensor,  $\boldsymbol{\tau}$  is the viscous stress tensor,  $\mathbf{n}$  is the unit normal vector,  $\boldsymbol{\sigma}$  is Cauchy stress tensor,  $\bar{\Psi}$  is the strain energy density function,  $I_i$  are the invariants and  $k_i$  are material parameters

To model the shear thinning behavior of blood with a dependence of hematocrit, the viscosity of blood was modelled using the Quemada models using literature published rheological parameters [7]. The relationship of the Quemada model is shown in equation (5). The four rheological parameters used in the Quemada model were kept constant for current study with  $\mu_{\text{plasma}}$ ,  $\dot{\gamma}_c$ ,  $k_0$ , and  $k_\infty$  equal to 1.28 mPa s, 4.2 s<sup>-1</sup>, 4.01, and 1.77, respectively [7].

$$\mu = \frac{\mu_{\text{plasma}}}{\left(1 - \frac{\text{Htc} \cdot k_{eq}}{2}\right)^2}, \text{ and } k_{eq} = \frac{k_0 + k_\infty \sqrt{\dot{\gamma}/\dot{\gamma}_c}}{1 + \sqrt{\dot{\gamma}/\dot{\gamma}_c}}, \quad (5)$$

Where  $\mu_{\text{plasma}}$  is the viscosity of blood plasma, Htc is the hematocrit,  $k_0$  and  $k_\infty$  are the maximum volume fraction at zero and infinite shear rates,  $\dot{\gamma}$  is the shear rate, and  $\dot{\gamma}_c$  is the critical shear rate for erythrocytes agglomeration

### B. Computational Model

3D idealized ascending thoracic aortic aneurysms, sectioning between the aortic sinus and brachiocephalic artery, were recreated based on echocardiogram measurements from three selected patients as shown in Fig. 1. Data extraction from these cases was approved by the Institution's Research Ethics Board.

Table 1 ATAA Measurements

	Inlet [mm]	Diameter [mm]	Outlet [mm]	Diameter [mm]	Inlet Peak Velocity [cm/s]
Case 1	45		44		160
Case 2	42		53		436
Case 3	48		40		389.3

The measurements of ATAA's diameter and peak velocity are presented in Table 1. The cases were selected based on the ratio between inlet and outlet diameter, with approximately same diameter for Case 1, larger outlet diameter for Case 2 and larger inlet diameter for Case 3.

The current finite element models were created with COMSOL Multiphysics® (V5.2, Stockholm, Sweden). The wall of the ATAA was modelled with uniform wall thickness of 2.59 mm. The aortic wall had a density of 1100 kg m<sup>-3</sup>, anisotropic material parameters of  $k_1 = 0.56$  MPa and  $k_2 = 16.21$ , isotropic material parameter of  $k_3 = 0.017$  MPa, and fiber crossing of  $\theta = 51^\circ$  [8].

The density of blood was 1060 kg m<sup>-3</sup> with two hematocrit values of 27%, and 44%. Blood flow inlet boundary received a fully developed time-dependent velocity profile with a matching case-specific peak flow velocity measured by echocardiogram. Both normotension (120/80 mmHg) and hypertension (160/90 mmHg) pressure conditions were applied to the flow outlet boundary. Additionally, to account for aortic wall expansion under cardiac cycle, the proximal/inlet end of the ATAA was applied with a fixed relative motion and the distal/outlet end was only constrained normally with respect to the cross-sectional plan. A total of five cardiac cycles of 75 beats per minute were solved using parallel sparse direct solver MUMPS (MULTifrontal Massively Parallel Sparse direct Solver) under a relative error less than 1e-3.

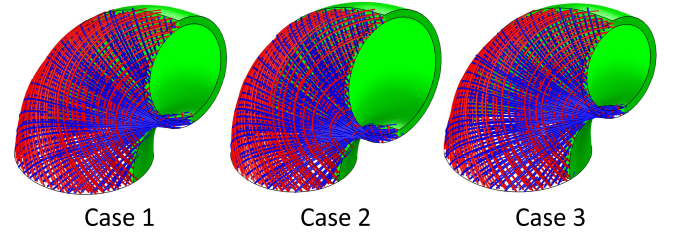


Fig. 1 Schematic representation of the computational domains with collagen fibers distribution

## III. RESULTS AND DISCUSSION

### A. Wall shear stresses

As the Quemada model captures the shear thinning behavior of blood, any region with lower shear rate within the aneurysm would lead to a higher blood viscosity. As the result, there would be differences in the shear stress distribution between normotension and hypertension, as well as between the hematocrits. In current analysis, the maximum shear stress magnitude along the wall (WSS) at peak systole was processed.

Table 2 Maximum WSS magnitude at peak systole

	Case 1 27%Htc	Case 1 44%Htc	Case 2 27%Htc	Case 2 44%Htc	Case 3 27%Htc	Case 3 44%Htc
Normotension [dPa]	86.6	143.9	248.9	449	320.8	640
Hypertension [dPa]	79.1	132.3	238.7	442.9	295.3	585

Given the similarity in WSS magnitude between normotension and hypertension, only the normotensive data over one cardiac cycle is shown in Fig. 2. The maximum WSS at peak systole are summarized in Table 2. Overall, there was an approximate 8% decrease in maximum WSS under hypertension for Case 1 and 3, and the decrease in WSS for Case 2 was smaller at 4.1% and 1.4% for 27% and 44% hematocrit (Htc), respectively. The WSS magnitude increased dramatically with the increase in hematocrit for all cases regardless of the blood pressure conditions. The approximate increase of WSS due to the increase of hematocrit, as shown in Fig. 2, is 40% (Case 1), 45% (Case 1) and 50% (Case 3).

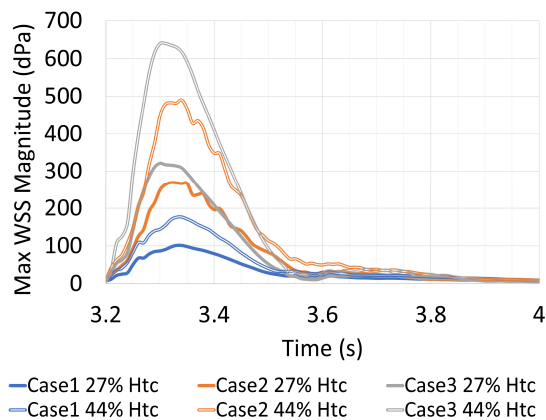


Fig. 2 Maximum wall shear stress magnitude over one cardiac cycle under normotension for three cases between two hematocrits

To better visualize the distribution of WSS and highlight the increase of stress with higher hematocrit, the contour plots for all cases are shown in Fig. 3 for normotension and in Fig. 4 for hypertension. The overall distributions of the elevated WSS for all cases are consistent. With the increase in hematocrit, the shear stress propagates to the upstream from the anterior and posterior side of the ATAA. Given that the blood cells and endothelial layers might respond to the elevated shear stress including shear induced platelet aggregation and thrombosis, the difference in patients' hematocrit values combining with the ATAA's anatomical configuration could be an additional assessment factor during an evaluation.

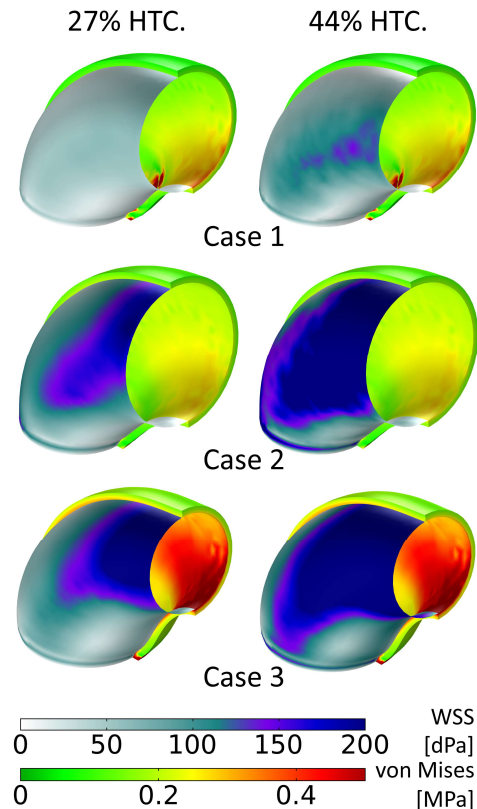


Fig. 3 Contours of von Mises stress along the arterial wall and wall shear stress under normotension

### B. Arterial wall stresses

In addition to the WSS distributions included in Fig. 3 and Fig. 4, the von Mises stresses within the arterial wall were also plotted. There were significantly increase in the stress distribution under the hypertensive condition; however, the variations between the hematocrits were minimum. The distribution of the von Mises stress along the internal arterial wall surface can be assessed by a threshold of 0.25 MPa.

Shown in Fig. 5 at peak systole of 3.3s, the majority of the ATAA wall experienced a stress less than 0.25MPa under normotension for both Case 1 and Case 2; however, a significant portion of Case 3 was under high wall stress. Between normotension and hypertension, there was significant increase in wall stress distribution for Case 2, followed by Case 1 then Case 3. These results were similar to the previous prediction made using blood as Newtonian fluid. With the increase in hematocrit, only Case 2 under hypertension had a minor increase in von Mises stress while all other cases remained relatively unchanged. The results suggested that the

stress experienced by the arterial wall were relatively independent from the change in hematocrit. The stress elevations were depended on both the blood pressure as well as the anatomical configurations of the aneurysm.

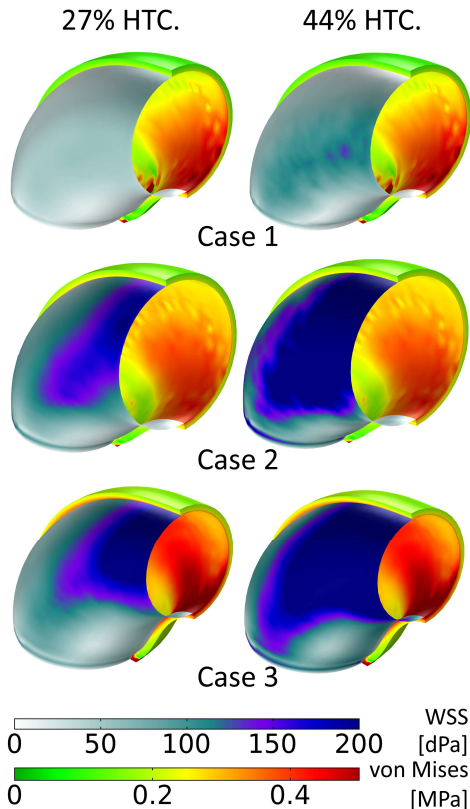


Fig. 4 Contours of Von Mises stress along the arterial wall and wall shear stress under hypertension

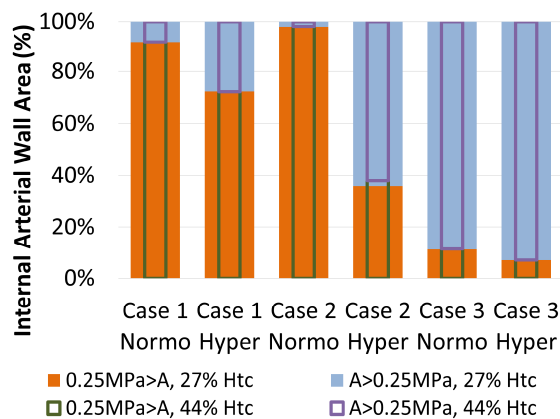


Fig. 5 Contours of Von Mises stress along the arterial wall and wall shear stress under hypertension

#### IV. CONCLUSIONS

The current study uses the fully coupled FSI method combined with the Quemada model for investigating the hemodynamics of ascending thoracic aortic aneurysm. By changing the hematocrit, which affected the degree of shear thinning of blood, the results suggested a significant increase in wall shear stress with the increase of hematocrit. On the other hand, the arterial wall stress distributions remained relatively independent from the changes of hematocrits.

#### ACKNOWLEDGMENT

The financial support of the Natural Sciences and Engineering Research Council (NSERC) of Canada is gratefully acknowledged. This research was enabled in part by the support provided by WestGrid ([www.westgrid.ca](http://www.westgrid.ca)) and Compute Canada ([www.computeCanada.ca](http://www.computeCanada.ca)).

#### CONFLICT OF INTEREST

The authors declare that they have no conflict of interest.

#### REFERENCES

- Rabkin, S. W. (2015). Accentuating and opposing factors leading to development of thoracic aortic aneurysms not due to genetic or inherited conditions. *Front Cardiovasc Med*, 2, 21.
- Davies, R. R., Goldstein, L. J., Coady, M. A., Tittle, S. L., Rizzo, J. A., Kopf, G. S., & Elefteriades, J. A. (2002). Yearly rupture or dissection rates for thoracic aortic aneurysms: simple prediction based on size. *Ann Thorac Surg*, 73(1), 17-28.
- García-Herrera, C. M., Celentano, D. J., & Herrera, E. A. (2017). Modelling and numerical simulation of the in vivo mechanical response of the ascending aortic aneurysm in Marfan syndrome. *Med Biol Eng Comput*, 55(3), 419-428.
- Roccabianca, S., Figueroa, C. A., Tellides, G., & Humphrey, J. D. (2014). Quantification of regional differences in aortic stiffness in the aging human. *J Mech Behav Biomed*, 29, 618-634.
- Yeh, H. H., Rabkin, S. W., & Grecov, D. (2018). Hemodynamic assessments of the ascending thoracic aortic aneurysm using fluid-structure interaction approach. *Med Biol Eng Comput*, 56(3), 435-451.
- Holzapfel, G. A., Gasser, T. C., & Ogden, R. W. (2000). A new constitutive framework for arterial wall mechanics and a comparative study of material models. *J Elasticity*, 61(1-3), 1-48.
- Marcinkowska-Gapińska, A., Gapinski, J., Elikowski, W., Jarczyk, F., & Kubisz, L. (2007). Comparison of three rheological models of shear flow behavior studied on blood samples from post-infarction patients. *Med Biol Eng Comput*, 45(9), 837-844.
- Weisbecker, H., Pierce, D. M., Regitnig, P., & Holzapfel, G. A. (2012). Layer-specific damage experiments and modeling of human thoracic and abdominal aortas with non-atherosclerotic intimal thickening. *J Mech Behav Biomed*, 12, 93-106.